

Original Article

Curcumin derivative WZ35 efficiently suppresses colon cancer progression through inducing ROS production and ER stress-dependent apoptosis

Junru Zhang^{1,2,3}, Zhiguo Feng¹, Chunhua Wang³, Huiping Zhou¹, Weidong Liu¹, Karvannan Kanchana¹, Xuanxuan Dai¹, Peng Zou¹, Junlian Gu^{2,4}, Lu Cai^{2,4}, Guang Liang¹

¹Chemical Biology Research Center, School of Pharmaceutical Sciences, Wenzhou Medical University, Wenzhou, Zhejiang 325035, China; ²Chinese-American Research Institute for Diabetic Complications, School of Pharmaceutical Science, Wenzhou Medical University, Wenzhou, Zhejiang 325035, China; ³School of Pharmaceutical Science, Binzhou Medical University, Yantai, Shandong 264003, China; ⁴Kosair Children's Hospital Research Institute, Department of Pediatrics of The University of Louisville, Louisville, KY 40202, USA

Received December 8, 2015; Accepted February 4, 2016; Epub February 1, 2017; Published February 15, 2017

Abstract: Colon cancer is characterized by its fast progression and poor prognosis, and novel agents of treating colon cancer are urgently needed. WZ35, a synthetic curcumin derivative, has been reported to exhibit promising antitumor activity. Here, we investigated the in vitro and in vivo activities of WZ35 and explored the underlying mechanisms in colon cancer cell lines. WZ35 treatment significantly decreased the cell viability associated with G2/M cell cycle arrest and apoptosis induction in colon cancer cell lines. We also show that WZ35 is highly effective in inhibiting tumor growth in a CT26 xenograft mouse model. Mechanistically, WZ35 treatment significantly induced reactive oxygen species (ROS) generation and endoplasmic reticulum (ER) stress in CT26 cells. Abrogation of ROS production by N-acetylcysteine (NAC) co-treatment almost totally reversed the WZ35-induced cell apoptosis and ER stress activation. Inhibition of p-PERK by GSK2606414 can significantly reverse WZ35-induced cell apoptosis in CT26 cells. Taken together, the curcumin derivative WZ35 exhibited anti-tumor effects in colon cancer cells both in vitro and in vivo, via a ROS-ER stress-mediated mechanism. These findings indicate that activating ROS generation could be an important strategy for the treatment of colon cancers.

Keywords: Colon cancer, curcumin derivative, reactive oxygen species, endoplasmic reticulum stress, apoptosis

Introduction

Colorectal carcinoma (CRC) is the third most common malignancy and the second most common cause of cancer death in the United States [1]. The advanced high-grade disease is correlated with increased metastasis and mortality with a five-year survival rate less than 10% [2, 3]. Current treatment includes surgical resection (debulking), followed by multi-agent chemotherapy, to provide almost no benefit because of the high recurrence rate, and a poor prognosis. The morbidity of CRC is increasing during recent years. However, the knowledge of treatments is still limited [4]. Thus new therapeutic strategies of improving survival for the patients with CRC are needed.

Curcumin, known as 1,7-bis(4-hydroxy-3-methoxyphenol)-1,6-heptadiene-3,5-dione, is obta-

ined and purified from a natural plant turmeric (*Curcuma longa*). It has been widely studied for its anti-inflammatory, anti-angiogenic, anti-oxidative, and anti-cancer effects in Indian and Chinese medicines [5]. Moreover, extensive research has shown that curcumin possesses anti-proliferative and anti-carcinogenic properties in a wide variety of cell lines and animals, partly due to its ability to arrest the cell cycle, induce apoptotic activity and inhibit the proliferation and metastasis of tumor cells [6, 7]. However its chemical instability and fast metabolism limits the clinical efficacy. [8]. Various approaches including chemical modification have been investigated to overcome the limitations of curcumin.

In the past several years, our lab has been engaged in the chemical modification of curcumin to design novel molecules with higher

chemical stability and stronger pharmacological effects than curcumin. Previously, a series of mono-carbonyl analogs of curcumin were synthesized and evaluated against various cancer cells [9]. Among them, compound 1-(4-hydroxy-3-methoxyphenyl)-5-(2-nitrophenyl)pent-1,4-dien-3-one (WZ35, **Figure 1A**) exhibited high chemical stability and good cancer activity. Here, we investigate the anti-cancer ability and mechanism of a curcumin analogue WZ35 in colon cancer cell lines. These results show that the anti-colon cancer action of WZ35 could be via the induction of intracellular reactive oxygen species (ROS) generation, resulting in the activation of endoplasmic reticulum (ER) stress-dependent cell apoptosis. Our study not only identifies WZ35 as a new candidate but also reveals that ROS activation may be a feasible strategy for the treatment of CRC.

Materials and methods

Materials and reagents

Curcumin was prepared in our lab. N-acetylcysteine (NAC) and 3-[4,5-dimethylthiazol-2-yl]2,5-diphenyltetrazolium bromide (MTT) were purchased from Sigma-Aldrich (St. Louis, MO). WZ35 (>98% purity, HPLC). Primary antibodies PERK, p-PERK (Thr980), p-eIF2 α , Cyclin B1, Cdc2, Bax, Bcl-2, cleaved PARP and horseradish peroxidase-conjugated goat anti-rabbit secondary antibody were purchased from Santa Cruz Biotechnology (Santa Cruz, CA). Antibodies ATF-4, CHOP, cleaved Caspase-3 and GAPDH were obtained from Cell Signaling Technology (USA).

Cell culture

Three types of colon cancer cell lines were purchased from the Institute of Biochemistry and Cell Biology, Chinese Academy of Sciences. Media RPMI-1640 for HCT116 and CT26 cells and DMEM for SW620 cells were used and supplemented with 10% fetal bovine serum (FBS, Invitrogen, USA), penicillin (100 units/mL) and streptomycin (100 μ g/ml) (Invitrogen, USA). Cells were grown at 37°C in a humidified atmosphere of 5% CO₂.

Assessment of cell viability by MTT assay

The viability of the cultured cells was determined by MTT assay. Briefly, cells were seeded in a 96-well plate. After culturing overnight,

cells were treated with the drugs for 24 h. Then 3-(4,5-Dimethylthiazol-2-yl)-2,5-diphenyltetrazolium bromide (MTT) (Sigma-Aldrich) solution (5 mg/ml) was added at the indicated time points, and cells were incubated for 4 h at 37°C in a humidified atmosphere (5% CO₂). Formazan formed in living cells was dissolved in dimethyl sulfoxide (DMSO) (Sigma-Aldrich), and absorbance of the solution was measured at 490 nm using a microplate reader (Reader 400 SFC, Lab Instruments, Hamburg, Germany).

Cell cycle analysis

All the three colon cancer cell lines were treated with or without WZ35 and curcumin for 18 h. The cells were harvested and washed twice with PBS, then fixed in ice-cold 70% (v/v) ethanol for 16 h at 4°C. Before analysis, cells were washed with PBS, stained with PI, and incubated for 30 min in darkness at 37°C, according to the manufacturer's instructions. The samples were analysed by flow cytometry (BD, FACS Calibur, San Jose, CA, USA) using Cell Quest software.

Measurement of apoptosis by flow cytometry

Annexin V-FITC apoptosis detection kits were used according to the manufacturer's instructions to measure apoptosis. Cells were incubated with or without WZ35 for 24 h, collected and washed with PBS, gently re-suspended in annexin V binding buffer, and incubated with annexin V-FITC/7-AAD. Flow cytometry was performed using CellQuest Pro software (BD Science Technology).

Measurement of intracellular reactive oxygen species

The level of intracellular ROS was quantified using a fluorescent probe 2070-Dichlorofluoresceindiacetate (DCFH-DA Invitrogen). 2070-Dichlorofluoresceindiacetate is able to diffuse through the cell membrane readily and is enzymatically hydrolyzed by intracellular esterases to generate nonfluorescent DCFH, which is rapidly oxidized to highly fluorescent DCF in the presence of intracellular ROS. After treatment with or without WZ35 and curcumin for 8 h, cells were harvested and incubated with 10 mmol/L DCFH-DA in dark at 37°C. After incubation for 30 min, cells were centrifuged, and the pellet was washed twice with ice-cold PBS and re-suspended in PBS, followed by flow

ROS induction contributes to colon cancer treatment

cytometric analysis using FL-1 as a detector. The fluorescence was analyzed using a FACSCalibur flow cytometer (BD Biosciences, CA).

Western blot analysis

Cells or tissue samples were lysed in lysis buffer. The lysates were then centrifuged, and the protein content was quantified. Whole protein (50 µg/lane) from each sample was separated via SDS-polyacrylamide gel electrophoresis (12-15%), and then transferred to a PVDF membrane (Millipore, UK), followed by immunoblotting with the corresponding antibodies. Non-specific binding was avoided by blocking the nitrocellulose membrane with 5% skimmed milk in TBST for 1.5 h. TBST was used to dilute primary and secondary antibodies. The membranes were incubated with the primary antibodies overnight at 4°C and in the secondary antibody for 1 h at room temperature. The signals were detected using a chemiluminescence kit (Bio-Rad). All the antibodies were obtained from Cell Signaling Technology and Santa Cruz Biotechnology (Santa Cruz, USA).

Immunofluorescence

Cells were grown in 35 mm-well chambered slides. Treated or untreated cells were fixed with paraformaldehyde (4%) and incubated with 100% methanol at -20°C for 5 min before blocking with 1% fetal bovine serum (FBS). Cells were then washed with cold PBS for 3 times and then incubated with respective primary antibodies overnight at 4°C; the next day the cells were washed with PBS for 3 times and incubated with fluorescein isothiocyanate (FITC) conjugated goat anti-rabbit IgG (Era or ERb) at RT for 1 h, and then washed again with PBS for three times. After washing, the cells were stained with DAPI at RT for 5 min in dark. Following incubation, the cells were washed twice with PBS and immediately visualized under fluorescence microscope (Zeiss LSM 700 confocal).

Electron microscopy

After treatment, the cells in 60-mm plates were collected and fixed in phosphate buffer (pH 7.4) containing 2.5% glutaraldehyde overnight at 4°C. The cells were postfixed in 1% OsO₄ at room temperature for 60 min, stained with 1% uranyl acetate, dehydrated through graded acetone solutions, and embedded in Epon. Aeras

containing cells were block mounted and cut into 70-nm sections, and examined with the electron microscope (H-7500, Hitachi, Ibaraki, Japan).

In vivo antitumor study

Animals: Five-week-old BalB/c female mice (18-22 g) purchased from Vital River Laboratories (Beijing, China) were used in the present investigation. Animals were housed at a constant room temperature with a 12 h:12 h light/dark cycle. Animals had free access to pellet food and water. All the procedures of laboratory animal care in research were approved by Wenzhou Medical University Policy on the Care and Use of Laboratory Animals.

Experimental design: BalB/c female mice were divided into four groups (10 mice per group). After subcutaneous inoculation of CT26 (5 × 10⁵ cells in 100 µL of PBS/mouse), mice developed palpable mass (tumor volume range 100-220 mm³). Animals received a single dose treatment as described below:

Group I served as control (Vehicle Oral); Group II received WZ35 (25 mg/kg Oral); Group III received WZ35 (50 mg/kg Oral); Group IV received Curcumin (50 mg/kg Oral);

Length and width of the tumor were measured with the help of a digital vernier caliper. Tumor volume of each animal was calculated using the following formula:

$$\text{Tumor volume (mm}^3\text{)} = \text{Length (mm)} \times [\text{Width (mm)}^2] \times 0.5$$

At the end of treatment, all the animals were sacrificed, and tumor specimens were excised, weighed and homogenized with protein isolating buffer. The homogenate was used for the assessment of cleaved Caspase 3 activity and cleaved PARP by western blot analysis. In addition, tumor specimens were fixed in neutral 10% buffered formalin (pH 7.2) for tunel staining.

TUNEL staining: Tunel staining was done with One-step TUNEL apoptosis detection kit (Beyotime, Shanghai, China) according to the manufacturer's instructions. The cancer tissue slices were put into xylene before different concentration of ethanol to deparaffinizing. After deparaffinizing incubated the slices with protease K (with no Dnase) for 30 min. Slices were washed with

ROS induction contributes to colon cancer treatment

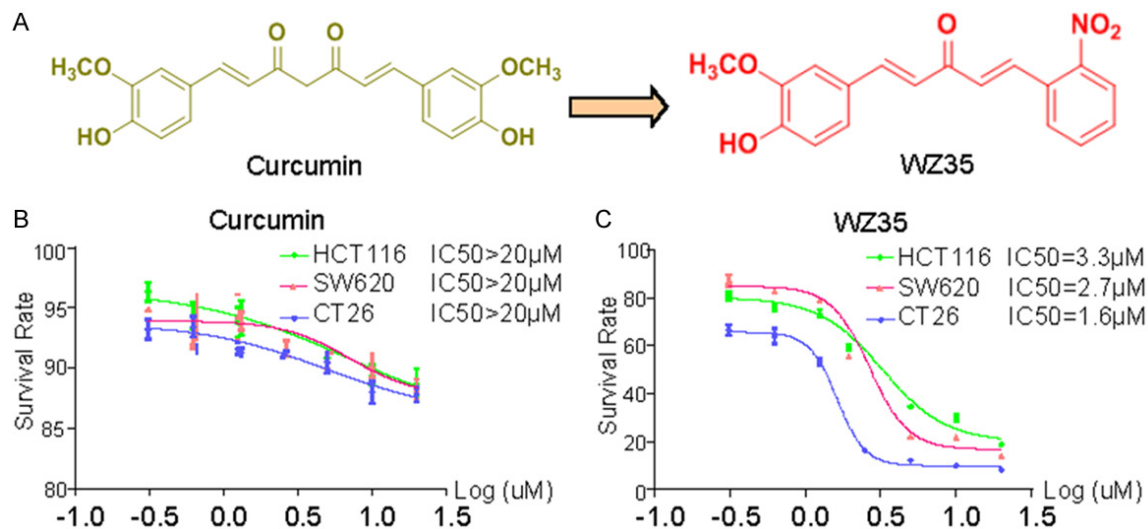


Figure 1. WZ35 inhibits cell proliferation of colon cells. A. Chemical structures of WZ35 and curcumin. B, C. Effects of WZ35 or curcumin on the proliferation of colon cancer cells. HCT116, SW620, or CT26 cells were incubated with increasing doses of WZ35 or curcumin (1.25–20 μ M) for 24 h, respectively. Cell viability was determined by MTT assay and the IC_{50} values were calculated.

PBS for 3 times and then incubated with tunnel detection of liquid at 37°C for 60 min in the dark. Slices were examined using a Nikon microscope.

Statistical analysis

Data were collected from at least 3 independent experiments for *in vitro* studies and 10 mice in each group for the *in vivo* studies, and were presented as mean \pm SD. ANOVA and Student's t-test in GraphPad Pro software (GraphPad, San Diego, CA) were used to analyze the statistical significance between sets of data. Differences were considered to be significant at $P < 0.05$.

Results

In vitro studies: WZ35 inhibited colon cancer cell proliferation and induced apoptotic death and cell cycle arrest

Using MTT assay, we evaluated the direct effect of WZ35 on the proliferation of colon cancer cell lines: HCT116, SW620 and CT26. Cells were treated with either vehicle (DMSO), increasing concentrations of WZ35 (μ M) or curcumin for 24 h. WZ35 exposure for 24 h significantly inhibited cell proliferation in a dose-dependent manner, with the IC_{50} values of 3.3 μ M (HCT116), 2.7 μ M (SW620), and 1.6 μ M (CT26), respectively (**Figure 1C**). Compared to the natural product curcumin, WZ35 showed

much stronger anti-proliferation activity (**Figure 1B**). In order to determine whether the cancer cell proliferation inhibition by WZ35 was associated with apoptosis, three kinds of colon cancer cells were treated with DMSO, WZ35 and curcumin for 24 h, and then were analyzed using Annexin V-FITC/PI-staining flow cytometry (**Figure 2A**). Quantitative results showed that treatment of colon cancer cells with different concentrations of WZ35 resulted in a significant increase in the number of apoptotic cells in a dose-dependent manner compared with curcumin and control group (**Figure 2B**). In addition, Western Blot analysis of cell apoptosis-regulatory molecules demonstrated that cleaved PARP, Bcl2, and Cleaved Caspase-3 were changed in all of three cancer cell lines treated with WZ35 for 24 h in a dose-dependent manner, while 20 μ M curcumin treatment showed little effect on the levels of these proteins (**Figure 2C**).

We also examined whether WZ35 induced cell cycle arrest using PI-staining flow cytometry in three kinds of colon cancer cell lines. Exponentially growing colon cancer cells were treated with WZ35 (2.5, 5, and 10 μ M) and curcumin (20 μ M) for 18 h and then subjected to flow cytometry. As shown in **Figure 3A** and **3C**, the cells treated with WZ35 were arrested in the G2/M phase. Most of the untreated and curcumin treated colon cancer cells were in the S phase, while the cells treated with WZ35 (2.5,

ROS induction contributes to colon cancer treatment

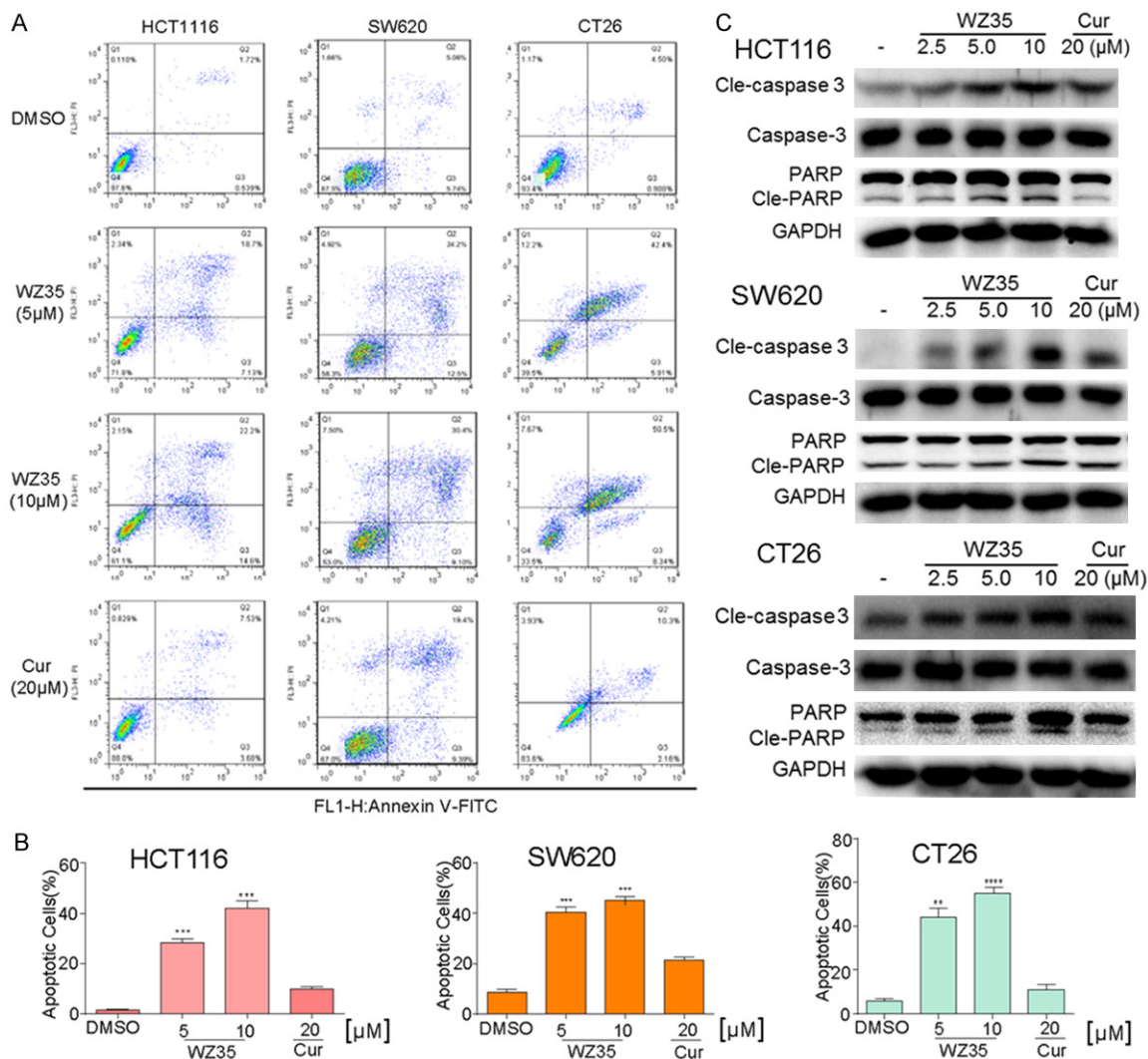


Figure 2. WZ35 induces apoptosis in colon cancer cells. A. Induction of apoptosis in colon cancer cells was determined by flow cytometry after treatment with WZ35 (5 μM or 10 μM) and curcumin (20 μM) for 24 h. Similar results were obtained in three independent experiments. B. The percentage of apoptotic cells in the treatment groups was calculated. C. The three colon cancer cells were treated with WZ35 (2.5, 5 or 10 μM) or curcumin (20 μM) for 24 h. Whole-cell lysates were subjected to western blot to assess the expression of cell apoptosis related proteins. GAPDH was used as internal control. Data represent similar results from three independent experiments. **p<0.01; ***p<0.001, vs DMSO group.

5, and 10 μM) showed a significantly greater proportion of cells in the G2/M phase in a dose-dependent manner. Similar results were observed in all three kinds of colon cancer cells. We then examined the expression of cell cycle-related proteins including MDM2, Cdc2, and Cyclin B1 by Western Blot analysis. Compared to the control and curcumin treated cells, the WZ35-treated cells exhibited dose-dependent decreases in the expression of MDM2, Cdc2, and Cyclin B1, which is consistent with the role of these proteins in the regulation of cell cycle (Figure 3B).

In vivo study: WZ35 significantly inhibits CT26 cell growth in mouse models

To validate the antitumor effect of WZ35 *in vivo*, tumor xenografts transplanted by mouse colon cancer CT26 cells were used. It was found that the tumor volume in saline-treated mice was time-dependent increased, 50 mg/kg curcumin-treated tumor-bearing mice exhibited significant tumor inhibitory effects from post-treatment day 10 to 14 (Figure 4A), compared to which tumor-bearing mice treated with WZ35 at both 25 and 50 mg/kg showed much

ROS induction contributes to colon cancer treatment

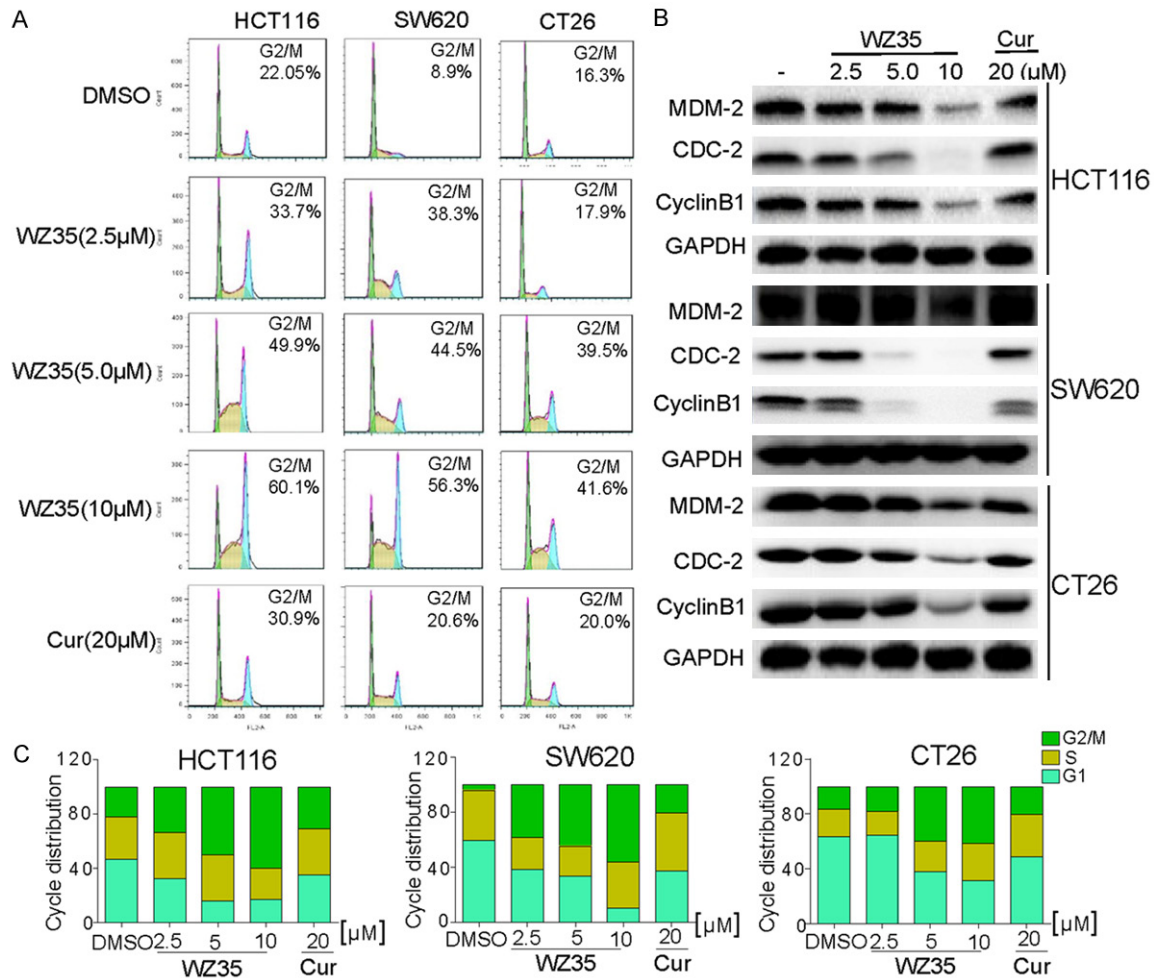


Figure 3. WZ35 induces cell cycle arrest in colon cancer cells. A. Induction of cycle arrest in colon cancer cells was determined by flow cytometry after treatment with WZ35 (2.5 μM, 5 μM or 10 μM) and curcumin (20 μM) for 18 h. Similar results were obtained in three independent experiments. B. Expression of cell cycle relative proteins were determined by western blot after treatment with WZ35 (2.5, 5.0 or 10 μM) or curcumin (20 μM) for 18 h. GAPDH was used as internal control. C. The ratio of different cells phase was determined via GraphPad Prism.

better tumor suppressive effect (**Figure 4A**). Sizes of the tumors in mice treated with WZ35 were visibly much smaller than those in control and treated with curcumin (**Figure 4B**). The result demonstrated that WZ35 significantly inhibited tumor growth during the 2-week treatment. This result was further confirmed by quantitative analysis of the tumor weights (**Figure 4C**). In addition, none of the mice died during the treatment and the body weight of the mice was similar among all groups during the period of 14-day treatment, indicating a good safety profile of WZ35 at the indicated dosages (**Figure 4D**). Western Blot and immunohistochemistry analysis using the tumor tissues revealed treatment with WZ35 at both dose levels significantly increased the expression of cleaved-PARP and cleaved-Caspase 3 in the

tumor tissues compared to the vehicle and curcumin groups (**Figure 4F**). Correspondingly, an increased incidence of TUNEL-positive cells was observed in the tumor tissues of WZ35-treated mice in comparison with the tumor tissues taken from vehicle and curcumin treated mice (**Figure 4E**). These data are consistent with anti-proliferation activities of WZ35 *in vitro*. In addition, WZ35 had more potent anti-tumor activity than curcumin *in vivo*.

Mechanistic study: WZ35 induces colon cancer apoptotic death via evoking ROS generation and ER stress-related cell death pathway

Overproduction of ROS can induce apoptosis through both extrinsic and intrinsic pathways. Curcumin was reported to induce apoptosis by

ROS induction contributes to colon cancer treatment

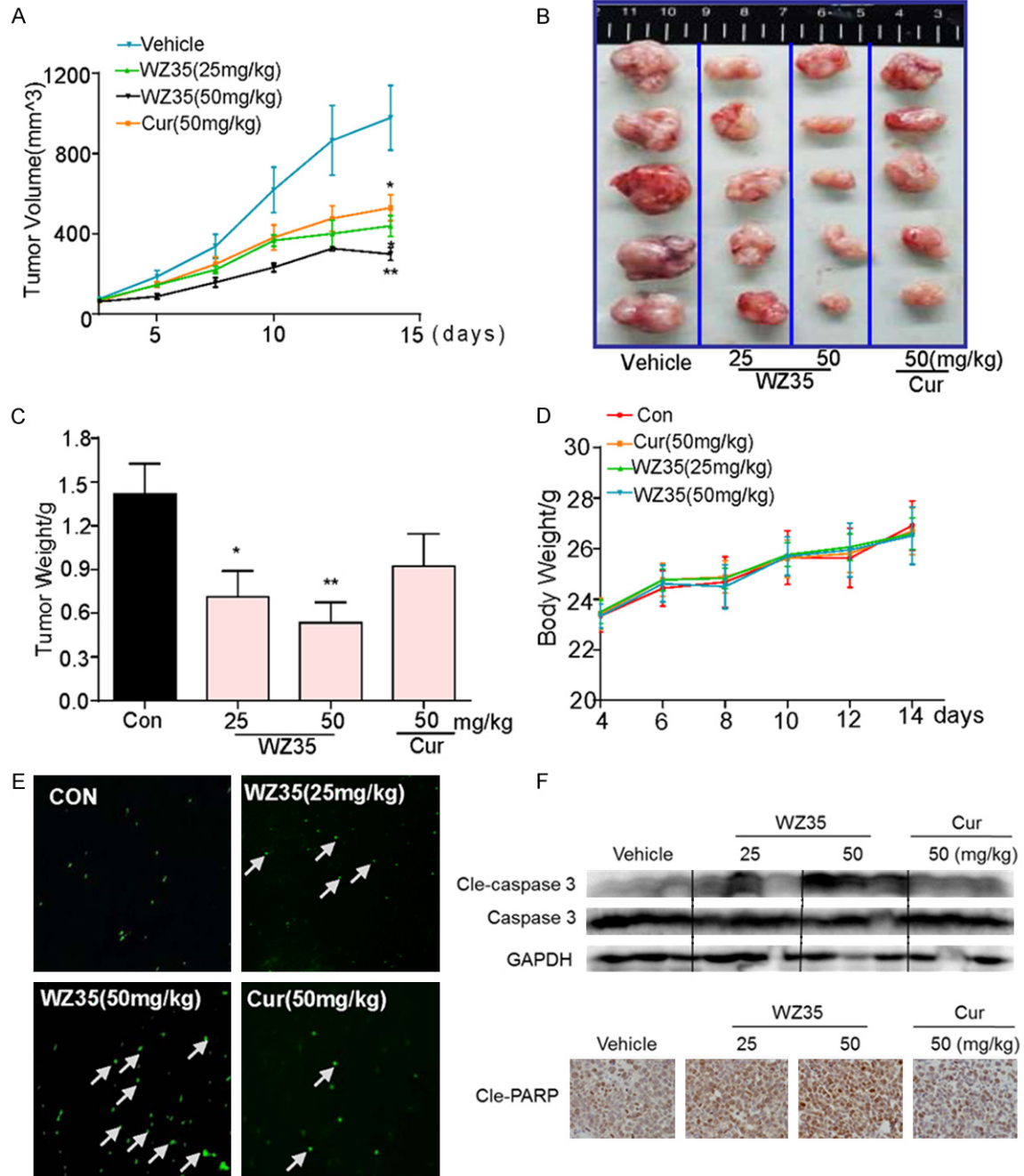


Figure 4. WZ35 inhibits colon cancer tumor xenograft growth in vivo. A. Tumor volumes in WZ35 and curcumin treated mice were smaller than those of vehicle treated mice. CT26 cells were injected to the flaks of Balb/C mice and the tumors were allowed to develop for 14 d. Subsequently, Balb/C mice bearing CT26 xenografts received WZ35 orally at the dose of 25 or 50 mg/kg or 50 mg/kg curcumin for a total of 14 days. Tumor volume was monitored. B, C. On day 14, tumors were excised and subjected to weight analysis. D. Body weight of the Balb/C mice in vehicle treated, WZ35 treated and curcumin treated mice. E. Tumor sections were performed for TUNEL staining analysis to detect apoptotic cells. F. Western blot analysis on the expressions of caspase 3, GAPDH was used as protein loading control, and tumor sections were stained with an anti-Cle-PARP Ab to detect PARP cleavage from respective tumor tissue. * $p < 0.05$; ** $p < 0.01$, vs control group.

stimulating the ROS formation [10]. WZ35-treated cells showed an increased ROS production in a dose-dependent manner (Figure 5A).

Pre-treatment of CT26 cells with a ROS inhibitor NAC, before the WZ35 treatment, completely blocked the WZ35-induced generation of

ROS induction contributes to colon cancer treatment

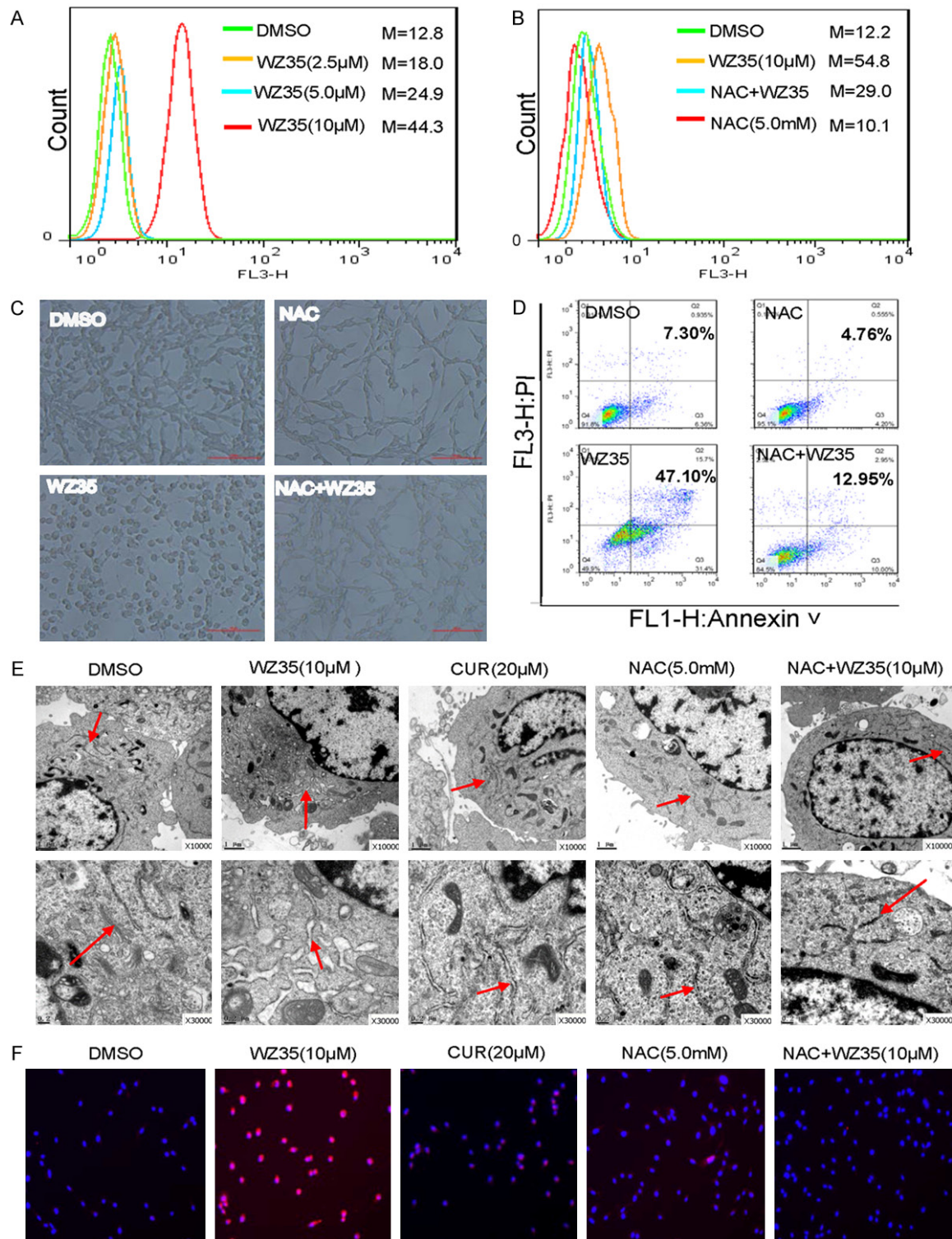


Figure 5. WZ35 induces cytotoxicity in colon cancer cells is dependent on intracellular ROS generation and subsequent ER stress activation. A. Intracellular ROS generation induced by increasing doses of WZ35 was measured in CT26 cells by staining with DCFH-DA (10 μ M) and flow cytometry analysis. B. CT26 cells were pre-incubated with 5 mM NAC for 1 h before exposure to WZ35 (10 μ M) for 8 h. Intracellular ROS generation was measured by flow cytometry. C. Blocking of ROS generation CT26 Cells were pre-incubated with or without 5 mM NAC for 1 h before exposure to WZ35 (10 μ M) for 24 h. Cell shape was observed. D. CT26 cells were pretreated with or without 5 mM NAC for 1 h before exposure to WZ35. Percentage of cell apoptosis was determined by Annexin-V/PI staining and flow cytometry. E. Effect of WZ35 on the morphology of endoplasmic reticulum in CT26 cells. Cells were pre-incubated with or without 5 mM NAC for 1 h before exposure to WZ35 (10 μ M) for 4 h. The morphology of endoplasmic

ROS induction contributes to colon cancer treatment

reticulum in CT26 cells was examined with an electron microscope ($\times 10000$ or $\times 30000$). F. Effect of WZ35 on CHOP expression in CT26 cells. Cells were pre-incubated with or without 5 mM NAC for 1 h before exposure to WZ35 (10 μ M) for 12 h. The fluorescence of CHOP was observed through immunostaining and fluorescence microscope.

ROS as shown by DCF fluorescence assay (**Figure 5B**). We also measured the apoptotic cell rates using cell morphology and flow cytometry in cancer cells treated with WZ35 alone, and cancer cells pre-incubated with NAC. The robust down-regulation of apoptotic cell rate observed in cells with the NAC pre-incubation further supports that ROS is involved in the induction of apoptosis (**Figure 5C, 5D**).

Having clearly established that WZ35 can induce apoptosis at least partially via induction of ROS production in colon cancer cells, we further investigated the underlying molecular mechanism of the cell death and ROS role in CT26 cell lines. ER stress has been considered as a major pathway for ROS-mediated cell death [11]. We first examined the effect of WZ35 on the morphology of ER in CT26 cells by electron microscopy. **Figure 5E** shows that ER was smooth (the arrow) in vehicle-treated CT26 cells, while 4 h after the treatment with WZ35 (10 μ M), the ER in CT26 cells became swelling (arrow), suggesting the accumulation of misfolded protein in ER. NAC pretreatment could totally block the ER swelling (**Figure 5E**). CHOP is a hallmark in ER stress activation and ER stress-induced apoptosis. We then determined the CHOP expression in CT26 cells treated with WZ35/NAC by immunofluorescence. **Figure 5F** depicts that WZ35 treatment significantly increased CHOP expression, while pretreatment with NAC completely abrogated the CHOP induction in CT26 cells. These results demonstrate that WZ35 could activate ER stress in CT26 cells, which is mediated by ROS generation.

We further analyzed the expression of the following key signal transduction molecules in pro-apoptotic ER stress pathway: protein kinase RNA (PKR), ER kinase (PERK), eukaryotic initiation factor 2 (eIF2 α), activating transcription factor 4 (ATF4), and growth arrest and DNA damage-inducible gene 153 (GADD153/CHOP). Expressions of p-PERK and p-eIF2 α increased in 1 h upon the WZ35 treatment (**Figure 6A**), so were for ATF4 in 3-6 h and CHOP in 12 h upon the WZ35 treatment (**Figure 6A**). The time sequence is consistent with the notion that ATF4 is an upstream mediator of CHOP and downstream effector of P-PERK and p-eIF2 α . Then

we carried out the WZ35 dose-effect study for the expression of these four proteins in CT26 cells. WZ35 treatment for respective time dose-dependently increased the expression of p-PERK, p-eIF2 α , ATF-4, and CHOP, while treatment with curcumin at 20 μ M showed slightly activation of ER stress (**Figure 6B**). The data also show that the WZ35 induced a time-series cascade activation of p-PERK and p-eIF2 α in 1 h, ATF-4 in 3-6 h, and CHOP in 12 h.

Given that CHOP and ATF4 are key proteins in the ER stress pathway, next we tested whether the induction of ER stress is also related to WZ35-stimulated ROS generation. We pretreated the cells with 5 mM NAC 1 h prior to the treatment of WZ35. The results show that pre-incubation with NAC completely blocked the expression of CHOP induced by WZ35, and significantly attenuated the expression of ATF4 (**Figure 6C**), indicating the causative of ROS for the WZ35-induced ER stress. To determine whether ER stress is a direct cause for WZ35 to induce apoptotic death in colon cancer cells, a small PERK inhibitor GSK2606414 was used. After pre-incubation with GSK2606414, PERK phosphorylation was significantly reduced in WZ35-treated cells, so was the overexpression of its down-stream effector CHOP (**Figure 6D**). The down-regulation of p-PERK and CHOP by GSK2606414 in WZ35-treated cells resulted in a high survival rate of CT26 cells compared with the group that was treated with WZ35 alone (**Figure 6E**). Such results indicate that ER stress signaling activation at least partly mediated the CT26 cell apoptosis induced by WZ35.

Discussion and conclusions

As one of the most common malignant tumors, colon cancer is characterized by its fast progression and poor prognosis. Currently, though surgical operation is the main effective treatment option for colon, assisted therapies such as chemotherapy and radiotherapy are still indispensable, especially for patients at advanced stage [12]. Extensive efforts have been put on discovering new targets and molecular pathways to develop novel drugs. Curcumin has been widely reported for its anti-cancer properties in various cancers. However, poor pharmacokinetic profiles limit its clinical application. In

ROS induction contributes to colon cancer treatment

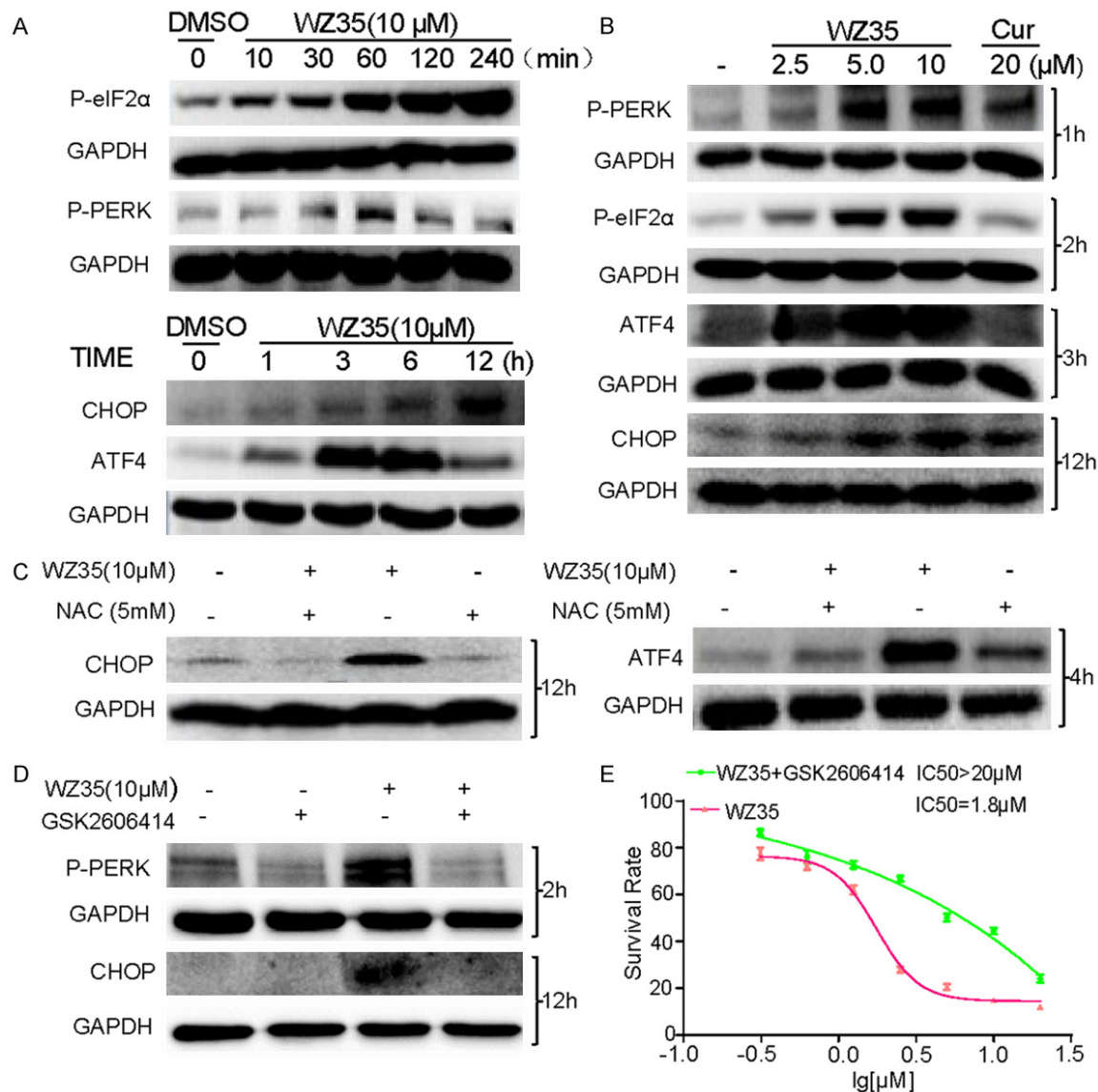


Figure 6. ER stress is involved in WZ35-induced colon cancer cells apoptosis. A. CT26 cells were treated with WZ35 (10 μ M) for different time, the protein levels of P-eIF2 α , P-PERK, ATF4 and CHOP were determined by western blot. B. CT26 cells were treated with WZ35 (2.5, 5 or 10 μ M) or curcumin (20 μ M) for indicated time, the expression of p-eIF2 α , p-PERK, ATF4 and CHOP were detected by western blot. GAPDH was used as internal control. C. CT26 cells were pre-incubated with 5 mM NAC for 1 h before treated with WZ35 (10 μ M) for 4 or 12 hours. The expression of ATF-4 or CHOP was detected by western blot assay. D. CT26 cells were incubated with p-PERK inhibitor (GSK2606414), the expression of p-PERK or CHOP in CT26 cells was determined by western blot after stimulation with WZ35 (10 μ M) for 2 h or 12 h. E. CT26 cells were pre-incubated with 2 μ M GSK2606414 for 2 h before treated with WZ35 or were only treated with WZ35 for 24 h. Cell viability was determined by MTT assay.

the present study, we investigated the effects of WZ35, an analog of curcumin, on colon cancer cells and xenograft tumors, as well as the underlying signaling pathways and mechanisms. The results show that WZ35 had excellent anticancer effects against colon cancer both *in vitro* and *in vivo*, possibly via inducing ROS production to trigger ER stress-dependent apoptosis, accompanied with cell cycle arrest.

Although curcumin has been reported to be able to induce a broad range of cancer cell death both the *in vitro* and *in vivo*, it only showed a modest inhibition of colon cancer cell proliferation *in vitro* in this study (Figure 1C). Previously, we have demonstrated that WZ35 is a chemically stable mono-carbonyl analog of curcumin that has anti-proliferative effects in gastric cancer cell lines [13]. Here, we found

that WZ35 was much more potent than curcumin in inducing cell apoptosis (**Figure 2**) and cell cycle arrest (**Figure 3**) in all three colon cancer cell lines. **Figure 3** suggests that WZ35 could induce G2/M phase cell cycle arrest in colon cancer cell lines, which is consistent with the result in gastric cancer cells [13]. Strikingly, treatment with WZ35 dramatically suppresses the expression of MDM-2, CyclinB1 and Cdc2, all of which are correlated with the cell cycle arrest (**Figure 3**). Coincide with the cell cycle arrest, the activation of Caspase-3 and PARP were also observed in the cell apoptosis induced by the WZ35 treatment in all three colon cancer cell lines (**Figure 2**). Compared with WZ35, curcumin (20 μ M) showed much less potent anti-cancer effects on both cell cycle arrest and apoptosis.

ROS are highly reactive oxygen free radicals and mainly originated from NADPH oxidase (NOX) and mitochondria [14]. ROS act as important multi-faceted signalling molecules that regulate multiple cellular pathways and play key roles in cell fate determination [15]. It is well known that accumulation of ROS can result in oxidative stress, impairment of cell function, and necrosis or apoptosis. Accumulating evidence suggest that the excessive oxidative stress could be an effective strategy to eliminate cancer cells [16]. Agents with the potential of inducing ROS generation have demonstrated anti-cancer effects in colon cancer cells [17-19]. Previous studies have demonstrated that ROS production play a vital role in curcumin-triggered apoptosis in some cells [20]. Herein, an increased ROS production was also observed in the WZ35-treated CT26 cells (**Figure 5A** and **5B**). Importantly, abrogation of ROS production by NAC co-treatment almost totally reversed the WZ35-induced cell apoptosis, suggesting a significant role of ROS in mediating WZ35-induced cell death (**Figure 5C**, **5D**). Our results further validated that the induction of ROS could be a good strategy for colon cancer therapy.

After ROS overproduction, a series of pro-apoptotic signaling pathways including ER stress were activated [21]. ER stress is a highly conserved cellular defense mechanism that responds to perturbations of ER function [22]. ROS can be an essential event that leads to protein misfolding in ER and ER stress-induced apoptosis [23]. Through the initiation of ER stress, ROS can affect a broad range of cellular

pathways including modulate cell cycle arrest, cell differentiation and canonical apoptotic pathways [24]. We also found that blockage of ROS production by NAC totally blocked WZ35's induction of ER stress activation (**Figures 5E**, **5F** and **6C**). In addition, ER stress-induced cancer cell apoptosis becomes an important signaling target for development of cancer therapeutic drugs [25]. The inductions of cancer cell apoptosis by some anti-cancer agents such as paclitaxel [26], farnesol [27] and polyphyllin D [28] have been reported to be mediated by ER stress. These observations in turn raised the question of whether or not the pro-apoptotic action of WZ35 is associated with ER stress signalling pathways mediated by ROS.

Prolonged activation of unfolded protein response (UPR) leads to excessive ER stress, and activates apoptotic pathways in mammalian cells [29]. Once the UPR signaling pathway is activated, PERK, which is a typical member of UPR, is activated and then phosphorylates the subunit of eIF2 α [30]. Phosphorylation of eIF2 α up-regulates ATF4 expression. In the commitment phase of ER stress-induced apoptosis, signaling through ATF-4 can trigger pro-apoptotic signals via activation of downstream transcriptional factor CHOP, triggering ER stress-specific cascade for implementation of cell apoptosis [31]. Recently, it was reported that curcumin exerts pro-apoptotic effects by inducing endoplasmic reticulum (ER) stress in human leukemia HL-60 cells [32], human lung carcinoma NCI-H460 cells [33], A549 cells and mouse melanoma cells [34]. To confirm whether WZ35-induced cell apoptosis is ER stress-related, we evaluated the effect of WZ35 on the morphology of ER in CT26 cells. Our data show that treatment with WZ35 (10 μ M) for 4 h induced a significant swelling of the ER in CT26 cells, suggesting an accumulation of misfolded protein in ER (**Figure 5E**). Using western blot analysis, we found a time-dependent activation of ER stress-related pro-apoptotic signaling, including p-PERK and p-eIF2 α (1 h treatment), ATF-4 (3-6 h treatment), and CHOP (12 h treatment) in WZ35-treated CT26 cells. These results show that the WZ35 induced ER stress from initiation to commitment, and finally to execution of ER stress-related apoptosis in a time-dependent manner (**Figure 6**). Therefore, ER stress was possibly involved in WZ35-induced colon cancer cell apoptosis. We further examine whether or not WZ35-induced cell apoptosis is ER stress-dependent. CT26 cells

were pre-treated with a PERK inhibitor. Inhibition of p-PERK by GSK2606414 can significantly inhibit WZ35-induced CHOP expression and cell apoptosis in CT26 cells, suggesting that the anti-tumor effects of WZ35 is at least partially ER stress-dependent (**Figure 6D** and **6E**). In addition, the results in **Figure 6E** suggest that ER stress is not the sole ROS-downstream pathway mediating the effect of WZ35.

The activation of ROS-mediated apoptosis in cancer cells may open up the possibility to extend the therapeutic options for WZ35 in colon cancer treatment. Indeed, besides the cellular effects, we have shown that WZ35 is highly effective in inhibiting tumor growth in a CT26 xenograft mouse model (**Figure 4**). In addition, WZ35 exhibited a good safety profile (**Figure 4D**). Taken together, the novel compound WZ35 exhibited anti-tumor effects in colon cancer cells both *in vitro* and *in vivo*, via ROS-ER stress-mediated mechanism. These properties of WZ35 could be further explored in the development of effective anticancer agents for the treatment of human colon cancer. The findings also indicate that activating ROS generation could be an important strategy for the treatment of colon cancers. However, despite the current data, the direct molecular target and the ROS-producing mechanism of WZ35 remain unclear. Therefore, further studies are necessary to establish this concept definitively, and to evaluate the *in vivo* pharmacodynamics of WZ35 as a candidate.

Acknowledgements

This work was supported by National Natural Science Foundation of China (81572448, 81-270489, and 81503107), Zhejiang Provincial Natural Science Foundation (LY16H310011), and Zhejiang Key Health Science and Technology Project (WKJ2013-2-021).

Disclosure of conflict of interest

None.

Authors' contribution

J.Z., Z.F., C.W., W.L., P.Z., and X.D. researched data; G.L. and H.Z. contributed initial discussion of the project; L.C. and J.G. reviewed the article; G.L. and K.K. wrote the article.

Address correspondence to: Dr. Guang Liang, Chemical Biology Research Center, School of Pharmaceutical Sciences, Wenzhou Medical University, Wenzhou 325035, China. Tel: +86-577-8668-9983; Fax: +86-577-86689983; E-mail: wzmcliang-guang@163.com; Dr. Lu Cai, Chinese-American Research Institute for Diabetic Complications, School of Pharmaceutical Science, Wenzhou Medical University, Wenzhou 325035, Zhejiang, China. Tel: +86-577-86699892; Fax: +86-577-86689982; E-mail: LOcai001@louisville.edu

References

- [1] Fleming M, Ravula S, Tatischev SF and Wang HL. Colorectal carcinoma: Pathologic aspects. *J Gastrointest Oncol* 2012; 3: 153-173.
- [2] Jeong KE and Cairns JA. Review of economic evidence in the prevention and early detection of colorectal cancer. *Health Econ Rev* 2013; 3: 20.
- [3] Wang J, Wang XY, Lin SY, Chen CD, Wang CR, Ma QY and Jiang B. Identification of Kininogen-1 as a Serum Biomarker for the Early Detection of Advanced Colorectal Adenoma and Colorectal Cancer. *PLoS One* 2013; 8: e70519.
- [4] Mishra J, Drummond J, Quazi SH, Karanki SS, Shaw JJ, Chen B and Kumar N. Prospective of colon cancer treatments and scope for combinatorial approach to enhanced cancer cell apoptosis. *Crit Rev Oncol Hemat* 2013; 86: 232-250.
- [5] Rahmani AH, Al Zohairy MA, Aly SM and Khan MA. Curcumin: A Potential Candidate in Prevention of Cancer via Modulation of Molecular Pathways. *Biomed Res Int* 2014; 2014: 761608.
- [6] Freudlsperger C, Greten J and Schumacher U. Curcumin induces apoptosis in human neuroblastoma cells via inhibition of NF kappa B. *Anticancer Res* 2008; 28: 209-214.
- [7] Subramaniam D, May R, Sureban SM, Lee KB, George R, Kuppusamy P, Ramanujam RP, Hideg K, Dieckgraefe BK, Houchen CW and Anant S. Diphenyl difluoroketone: A curcumin derivative with potent *in vivo* anticancer activity. *Cancer Res* 2008; 68: 1962-1969.
- [8] Puglia C, Cardile V, Panico AM, Craschi L, Offerta A, Caggia S, Drechsler M, Mariani P, Cortesi R and Esposito E. Evaluation of monooleine aqueous dispersions as tools for topical administration of curcumin: Characterization, *in vitro* and *ex-vivo* studies. *J Pharm Sci* 2013; 102: 2349-2361.
- [9] Liang G, Shao LL, Wang Y, Zhao CG, Chu YH, Xiao J, Zhao Y, Li XK and Yang SL. Exploration and synthesis of curcumin analogues with improved structural stability both *in vitro* and *in*

ROS induction contributes to colon cancer treatment

- vivo as cytotoxic agents. *Biorg Med Chem* 2009; 17: 2623-2631.
- [10] Chang ZQ, Xing JC and Yu XC. Curcumin induces osteosarcoma MG63 cells apoptosis via ROS/Cyto-C/Caspase-3 pathway. *Tumor Biol* 2014; 35: 753-758.
- [11] Xu XC, Liu TT, Zhang AM, Huo XX, Luo QL, Chen ZW, Yu L, Li Q, Liu LL, Lun ZR and Shen LL. Reactive Oxygen Species-Triggered Trophoblast Apoptosis Is Initiated by Endoplasmic Reticulum Stress via Activation of Caspase-12, CHOP, and the JNK Pathway in *Toxoplasma gondii* Infection in Mice (Retracted article. See vol. 83, pg. 1735, 2015). *Infect Immun* 2012; 80: 2121-2132.
- [12] Kolberg M, Holand M, Lind GE, Agesen TH, Skotheim RI, Hall KS, Mandahl N, Smeland S, Mertens F, Daudison B and Lothe RA. Protein expression of BIRC5, TK1, and TOP2A in malignant peripheral nerve sheath tumours - A prognostic test after surgical resection. *Mol Oncol* 2015; 9: 1129-1139.
- [13] Zou P, Zhang JR, Xia YQ, Kanchana K, Guo GL, Chen WB, Huang Y, Wang Z, Yang SL and Liang G. ROS generation mediates the anti-cancer effects of WZ35 via activating JNK and ER stress apoptotic pathways in gastric cancer. *Oncotarget* 2015; 6: 5860-5876.
- [14] Radak Z, Zhao ZF, Koltai E, Ohno H and Atalay M. Oxygen Consumption and Usage During Physical Exercise: The Balance Between Oxidative Stress and ROS-Dependent Adaptive Signaling. *Antioxid Redox Sign* 2013; 18: 1208-1246.
- [15] Zhou Y, Shu FR, Liang XY, Chang H, Shi LY, Peng XL, Zhu JD and Mi MT. Ampelopsin Induces Cell Growth Inhibition and Apoptosis in Breast Cancer Cells through ROS Generation and Endoplasmic Reticulum Stress Pathway. *PLoS One* 2014; 9: e89021.
- [16] Samoylenko A, Al Hossain J, Mennerich D, Kellokumpu S, Hiltunen JK and Kietzmann T. Nutritional Countermeasures Targeting Reactive Oxygen Species in Cancer: From Mechanisms to Biomarkers and Clinical Evidence. *Antioxid Redox Sign* 2013; 19: 2157-2196.
- [17] Doroshov JH, Gaur S, Markel S, Lu J, van Balgooy J, Synold TW, Xi BX, Wu XW and Juhasz A. Effects of idonionium-class flavin dehydrogenase inhibitors on growth, reactive oxygen production, cell cycle progression, NADPH oxidase 1 levels, and gene expression in human colon cancer cells and xenografts. *Free Radic Biol Med* 2013; 57: 162-175.
- [18] Park MH, Jo M, Won D, Song HS, Han SB, Song MJ and Hong JT. Snake venom toxin from *Vipera lebetina turanica* induces apoptosis of colon cancer cells via upregulation of ROS-and JNK-mediated death receptor expression. *BMC Cancer* 2012; 12: 228.
- [19] Maillat A, Yadav S, Loo YL, Sachaphibulkij K and Pervaiz S. A novel Osmium-based compound targets the mitochondria and triggers ROS-dependent apoptosis in colon carcinoma. *Cell Death Dis* 2013; 4: e653.
- [20] Liang T, Zhang XJ, Xue WH, Zhao SF, Zhang X and Pei JY. Curcumin Induced Human Gastric Cancer BGC-823 Cells Apoptosis by ROS-Mediated ASK1-MKK4-JNK Stress Signaling Pathway. *Int J Mol Sci* 2014; 15: 15754-15765.
- [21] Wang CL, Liu C, Niu LL, Wang LR, Hou LH and Cao XH. Surfactin-Induced Apoptosis Through ROS-ERS-Ca²⁺-ERK Pathways in HepG2 Cells. *Cell Biochem Biophys* 2013; 67: 1433-1439.
- [22] Jheng JR, Ho JY and Horng JT. ER stress, autophagy, and RNA viruses. *Front Microbiol* 2014; 5: 388.
- [23] Chaudhari N, Talwar P, Parimisetty A, d'Heilencourt CL and Ravanan P. A molecular web: endoplasmic reticulum stress, inflammation, and oxidative stress. *Front Cell Neurosci* 2014; 8: 213.
- [24] Farrukh MR, Nissar UA, Afnan Q, Rafiq RA, Sharma L, Amin S, Kaiser P, Sharma PR and Tasduq SA. Oxidative stress mediated Ca(2+) release manifests endoplasmic reticulum stress leading to unfolded protein response in UV-B irradiated human skin cells. *J Dermatol Sci* 2014; 75: 24-35.
- [25] Vaeteewoottacharn K, Kariya R, Matsuda K, Taura M, Wongkham C, Wongkham S and Okada S. Perturbation of proteasome function by bortezomib leading to ER stress-induced apoptotic cell death in cholangiocarcinoma. *J Cancer Res Clin Oncol* 2013; 139: 1551-1562.
- [26] Kawashima M and Kondo H. Comparison of Therapeutic G-CSF Cycles and Prophylactic G-CSF Cycles in Patients Receiving Paclitaxel and Carboplatin Combination Chemotherapy for Ovarian Cancer: A Retrospective Study Report. *J Rural Med* 2014; 9: 86-89.
- [27] Park JS, Kwon JK, Kim HR, Kim HJ, Kim BS and Jung JY. Farnesol induces apoptosis of DU145 prostate cancer cells through the PI3K/Akt and MAPK pathways. *Int J Mol Med* 2014; 33: 1169-1176.
- [28] Chan JYW, Koon JCM, Liu XZ, Detmar M, Yu BA, Kong SK and Fung KP. Polyphyllin D, a steroidal saponin from *Paris polyphylla*, inhibits endothelial cell functions in vitro and angiogenesis in zebrafish embryos in vivo. *J Ethnopharmacol* 2011; 137: 64-69.
- [29] Fabrizio G, Di Paola S, Stilla A, Giannotta M, Ruggiero C, Menzel S, Koch-Nolte F, Salles M and Di Girolamo M. ARTC1-mediated ADP-ribosylation of GRP78/BiP: a new player in endo-

ROS induction contributes to colon cancer treatment

- plasmic-reticulum stress responses. *Cell Mol Life Sci* 2015; 72: 1209-1225.
- [30] Guo XF and Yang XJ. Endoplasmic reticulum stress response in spontaneously hypertensive rats is affected by myocardial ischemia reperfusion injury. *Exp Ther Med* 2015; 9: 319-326.
- [31] Zhang X, Zhang HQ, Zhu GH, Wang YH, Yu XC, Zhu XB, Liang G, Xiao J and Li XK. A novel mono-carbonyl analogue of curcumin induces apoptosis in ovarian carcinoma cells via endoplasmic reticulum stress and reactive oxygen species production. *Mol Med Report* 2012; 5: 739-744.
- [32] Pae HO, Jeong SO, Jeong GS, Kim KM, Kim HS, Kim SA, Kim YC, Kang SD, Kim BN and Chung HT. Curcumin induces pro-apoptotic endoplasmic reticulum stress in human leukemia HL-60 cells. *Biochem Biophys Res Commun* 2007; 353: 1040-1045.
- [33] Wu SH, Hang LW, Yang JS, Chen HY, Lin HY, Chiang JH, Lu CC, Yang JL, Lai TY, Ko YC and Chung JG. Curcumin Induces Apoptosis in Human Non-small Cell Lung Cancer NCI-H460 Cells through ER Stress and Caspase Cascade- and Mitochondria-dependent Pathways. *Anticancer Res* 2010; 30: 2125-2133.
- [34] Bakhshi J, Weinstein L, Poksay KS, Nishinaga B, Bredesen DE and Rao RV. Coupling endoplasmic reticulum stress to the cell death program in mouse melanoma cells: effect of curcumin. *Apoptosis* 2008; 13: 904-914.